J8.3 STUDY OF SEA-BREEZE INTERACTIONS WHICH CAN PRODUCE STRONG WARM-SEASON CONVECTIVE WINDS IN THE CAPE CANAVERAL AREA

Christopher J. Ander, Adam J. Frumkin and James P. Koermer*
Plymouth State University, Plymouth, New Hampshire

William P. Roeder
45th Weather Squadron, Patrick Air Force Base, Florida

1. Introduction

As the primary provider of weather support to space launch operations at Cape Canaveral Air Force Station (CCAFS) and Kennedy Space Center (KSC), the USAF 45th Weather Squadron (45 WS) has a strong interest in improved forecasts of convective wind events, which can be hazardous to operations at the Florida Space Port (Harms et al. 1999). Convective wind warnings are the second most frequently issued warnings by 45 WS, lagging only behind lightning warnings. The 45 WS categorizes convective wind warnings as ≥35kt, ≥50kt, or ≥60kt from the surface to 300 feet. The Plymouth State University (PSU) research team has concentrated on improving the warm-season convective wind climatology for the area and developing other tools that can be used by 45 WS forecasters to address this problem.

This research by PSU has been conducted over the past 4 years with a different emphasis each year. The first year of this project created a warm-season downburst climatology for the CCAFS/KSC area covering 1995-2003. It was developed by Loconto et al. (2006) and focused primarily on identifying warning level events based on data gathered from the CCAFS/KSC wind tower network with over 40 sites (Figure 1). The wind towers measure 5 minute average peak wind speed from 12 ft to up to 497 Ft at up to 10 height levels (Case and Bauman 2004). This research analyzed only levels at 300 Ft or less to match the 45 WS warning requirements. Loconto's (2006) work also included analyzing surface data from KTTS the (Shuttle Landing Facility) upper air data from KXMR radiosonde observations as well as WSR-88D radar products from KMLB (Melbourne, FL) and satellite imagery. These data were used to examine common forecast techniques and thermodynamic indices, which were used to predict convective winds.

*Corresponding author address: Dr James P. Koermer, MSC #48, 17 High Street, Dept. of Atmospheric Science and Chemistry, Plymouth State University, Plymouth, NH, 03264; e-mail: koermer@plymouth.edu

The second year of the project focused primarily on analyzing the data set previously accumulated by Loconto (2006) and adding two additional years to 2005. Cummings et al. (2007) developed annual, monthly and diurnal distributions of warning level events for 1995 -2005. Additionally synoptic scale flow regimes were determined for each convective period. Flow regime classifications were based on the low level (1000 – 700mb) flow at the three closest upper air stations (KTBW, KJAX and KMIA), closely following a method developed in Lericos et al. (2002). The KXMR sounding was also used better define the thunderstorm flow regime by the NASA Applied Meteorology Unit (AMU) and Mr. Roeder of the 45 WS (Lambert and Roeder, 2008).

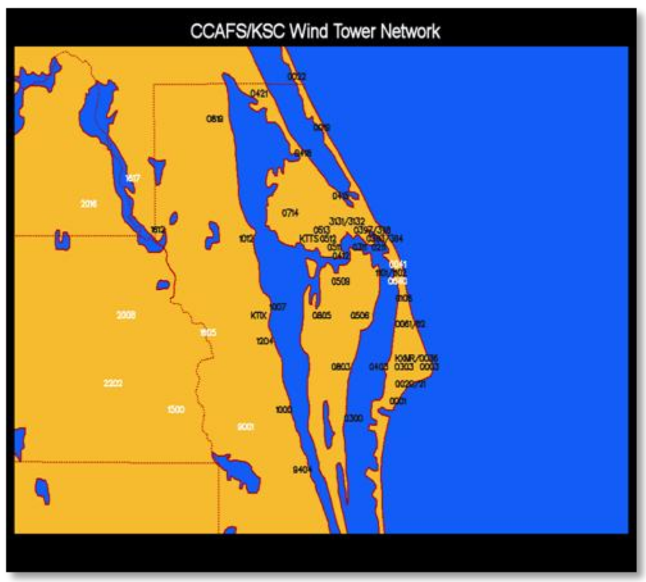

Figure 1. Map of the CCAFS/KSC wind towers and KTTS and KXMR. Only the stations in notated in black were used in this study.

During the third year of the project, Dinon et al. (2008) obtained and analyzed high resolution NEXRAD data from the National Climatic Data Center (NCDC) archive. These data consisted mainly of Melbourne (KMLB) 0.5° reflectivity which was used to determine cell strength, cell initiation, cell structure, group movement, cell movement and location of maximum peak wind with respect to the cell. This was only done for all warning level events for the eleven warm seasons between 1995 and 2005. These radar data were time-matched and overlaid with the corresponding peak wind tower data.

The most recent fourth year of the project has included updating the climatological statistics, originally developed by Cummings et al. (2007), and adding data for the years, 2006 and 2007. Additionally radar data were analyzed for all non-warning level convective events in the climatology. This eliminated a few previously identified convective cases and added a few new ones. The purpose of this paper is to compare and contrast non-warning level and warning level events with particular emphasis on the associated sea-breeze interactions.

2. Identification of Convective Periods

Convective periods were defined using a criteria defined by Cummings et al. (2007) as "a period of convective activity with at least a 6-hour break of no convection before and after the period. Start time was recorded at the top of the hour when convection first occurred and end time was noted at the top of the hour after the last evidence of convection."

High quality, detailed, manual surface observations from the NASA Shuttle Landing Facility (KTTS) were manually analyzed for reports of convection. Radar Control Message radar data obtained from the Plymouth State Weather Center (PSWC) were then used to confirm the proximity of convection to the CCAFS/KSC area and to refine the start and end times for each convective period. These periods were further refined using KMLB NEXRAD data retrieved from NCDC. Archived surface analyses of MSLP (contoured every 1 mb) overlaid with reported wind gusts were obtained from PSWC for each convective period and analyzed for days with strong synoptic scale forcing such as tropical cyclones or fronts; such days were eliminated from this study.

Table 1. Warm season convective period identification results for May-September from 1995-2007.

QUANTITY	Number	%
Total convective periods	872	100
Periods with winds ≥35 kt	305	35
Periods with winds ≥50 kt	61	7
Periods with winds ≥60 kt	11	1.2

As shown in Table 1, 35% of convective periods during the 13-year climatology produced warning criteria winds. Out of the average of 67 convective periods per warm-season, 43 of them (or 65%) were below warning thresholds, 24 of them (35%) had warning criteria winds. Of this latter category, annually 19 (or 28%) had peak winds in the range of 35-49 kt; 4 (5.6%) were in the 50-59 kt range; and only about 1 case (1.4%) per year was greater than or equal to 60 kt. The frequency distribution of peak speeds for all convective wind events and the best fit Gumbel curve are shown in Figure 2. It is interesting to note the years with relatively fewer convective periods tended to have a relatively greater frequency of warning-level events. The year 2006 had just 35 convective periods, the lowest in the climatology, yet 15 of them were warning criteria events. The maximum convective wind gust in the climatology, 74 kt, was also recorded in July of 2006.

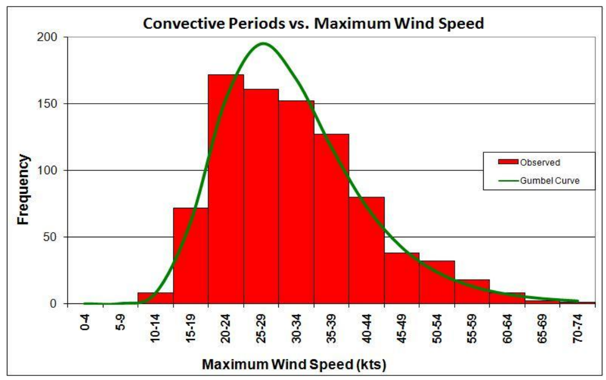

Figure 2. Peak speed frequency distribution and best fit Gumbel curve (1995-2007).

3. Data & Methods

Base Reflectivity data from KMLB were time matched and overlaid with wind tower reports from the CCAFS/KSC tower network. In the few cases with missing KMLB data, Tampa Bay (KTBW) data were used. Radar and wind data were displayed using a web interface capable of showing still images as well as loops. Previously, wind speed and direction were only represented by five digit numbers in the radar/wind overlay; recently options were added to represent the wind observations either using plotted wind barbs or streamlines. This update allowed sea-breeze and outflow boundaries to be indentified and tracked more easily and was also helpful in locating mesoscale areas of convergence prior to convective initiation. Streamlines often showed areas of convergence with cyclonic rotation that tended to move with strong reflectivity cores, i.e. strong updrafts. Examples of this web interface are shown in section 5.

Following Dinon et al. (2008), a radar/wind study was performed by analyzing the data for the variables of cell initiation, cell structure, cell strength, location of maximum peak wind (with respect to the cell thought to have produced the gust), group direction and individual cell direction. Specific definitions of these variables are contained in the Dinon et al. (2008) paper. Our study examined the years 2006 and 2007 for both warning level and non-warning level events and added non-warning level events from 1995 through 2005 to the climatology. The results from Dinon et al. (2008), pertaining to warning level events from 1995-2005 were used.

4. Results

4.1. Cell Initiation

Results indicate the significance of mesoscale boundary interactions in generating stronger, warning level events. For example, 68% of all warning level events in the climatology involved either a sea-breeze front, outflow boundary or a collision of the two while only 35% of all non-warning level events involved any of those boundary interactions (Figure 3). This is somewhat significant as only 47% of all cells (warning and non-warning) involve discernable mesoscale boundaries. This is reinforced by an analysis (Koermer and Roeder, 2008) that showed that the western most weather towers provided little warning of convective wind events for thunderstorms approaching from the west.

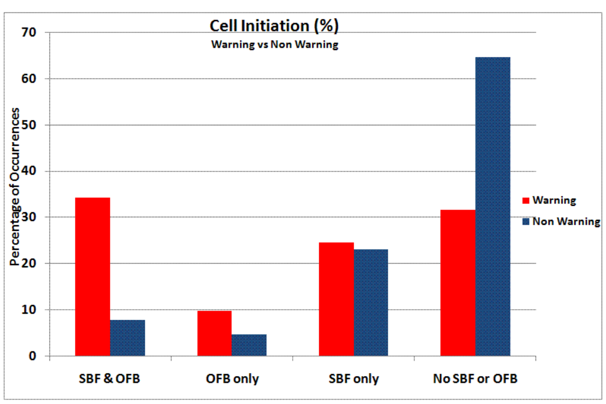

Figure 3. Cell Initiation with mesoscale boundaries with warning level cases are in red and non-warning level cases in blue. Initiation is shown on the x-axis and percentage of occurrence on the y-axis.

Apparently most of those storms do not generate downbursts until they are near or over the CCAFS/KSC. The interaction of the storms with local boundaries is a likely cause, especially the river breeze fronts from the Indian and Banana Rivers and the sea-breeze front, held close to the coast by the westerly flow regimes that lead to thunderstorms approaching from the west.

4.2. Cell Structure

There seems to be some correlation between the level of organization of the cells and the strength or their ability to produce warning level events. As figure 4 shows, almost 60% of warning level events resulted from linear cells, while cluster and individual cell structures account for the other 40%. Linear cell structure accounts for only 4.6% of all non-warning level events. Combining all warning and non-warning events, just 24% had linear cell structure. This further reinforces the idea that boundary interactions play an important role as sea-breeze and outflow boundaries were often observed to have a linear structure with cell's initiating along them. It was noted that there was an exceptionally large number of events in the "cluster" category overall. The physical mechanism for these results has not been investigated, but may be due to merging cells leading to stronger than average cells and/or boundary interaction with their own convective outflows.

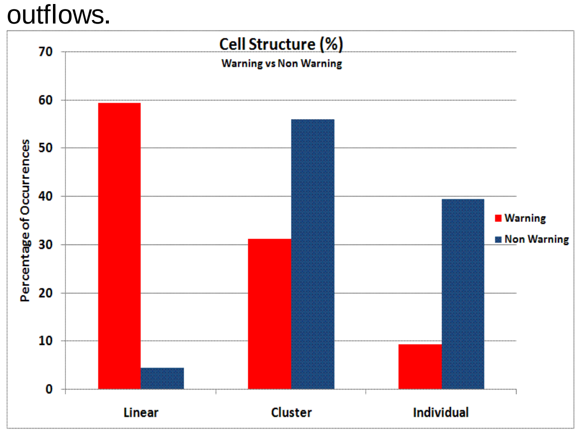

Figure 4. Cell structure with warning level in events shown in red and non-warning level cases in blue. Structure is shown on the x-axis and percentage of occurrence is shown on the y-axis.

4.3. Cell Strength

Warning level gusts result from "strong" cells 29% of the time while the "moderate" and "weak/broken" cell categories account for 53% and 18%, respectively (Figure 5). "Strong" cells make up 23% of all cells, while "moderate" and "weak/broken" account for 67% and 21% of all cells respectively. These results were somewhat surprising especially after comparing warning to non-warning criteria events. Also of note was that the “weak/broken” category contained an almost identical percentage of warning and non-warning level events. One hypothesis as to the relatively high number of warning level events in the weak/broken and moderate categories was the idea of collapsing storm cloud cores generating the downdraft with the strongest winds at the surface occurring slightly after the drop in radar reflectivity so that the reflectivity at the time of the peak winds is less than the reflectivity that drove the downburst.. The collapsing cores could explain the weaker reflectivity values at the time of peak wind. It was often observed that a cell would approach a tower at moderate or strong strength and become significantly weaker with reflectivity values dropping significantly just prior to the peak wind gust. This idea was suggested by Roeder as well as forecasters from the 45th Weather Squadron (personal communication, 2008).

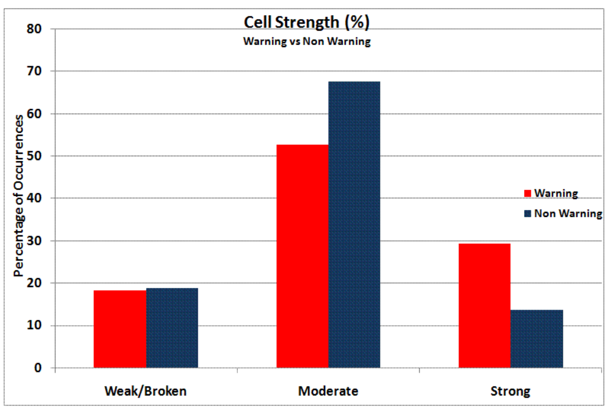

Figure 5. Cell strength with warning level events shown in red and non-warning level events in blue. Strength is shown on the x-axis and percentage of occurrence is shown on the y-axis.

4.4. Location with respect to max peak wind

Figure 6 shows that an overwhelming majority, 84%, of warning level wind gusts occur when the cell is located directly overhead or extremely close to the tower that recorded it. This is somewhat counterintuitive at first as downbursts winds are generally thought to propagate downshear of the cell. However, low to midlevel winds (1000-700 hPa) are often quite weak during the Florida warm season, which tends to lessen the horizontal propagation of winds from individual cells. This could potentially be more evidence supporting the collapsing core hypothesis. The majority of non-warning level winds were recorded at towers where the convection was well behind or well ahead of the tower. Frictional effects within the generally deep summertime boundary layer could have an effect of slowing winds significantly. Although a downburst may have been above warning criteria at the time of generation, it could have slowed down to below 35 kt by the time it reached a distant (5-10km) tower. This could explain the large percentage of non-warning level events that are seen in the ahead and behind categories. This idea could also help explain some of the counterintuitive results presented in section 4.3 where non-warning level events dominate the “moderate” (45-55 dBZ) cell strength category and are approximately equal in percentage to the warning events in the “weak/broken” category. “Warning” and “non-warning” level events are determined by the wind speed so this is likely an artifact of the above.

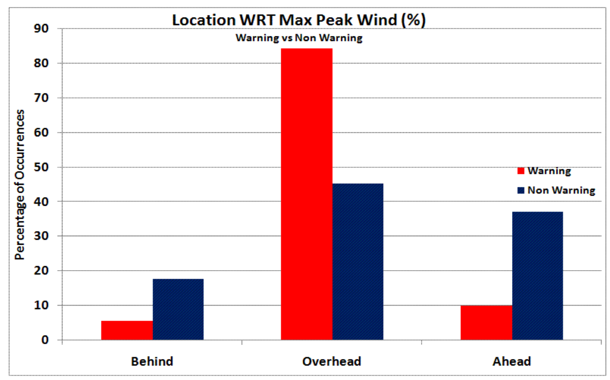

Figure 6. Location with respect to (WRT) Max peak wind with warning level events in red and non-warning level events in blue.

4.5. Cell Movement

Cell group movement and individual cell movement are considered separately in this section. An overall tendency for groups of cells to move east and individual cells embedded in the groups to move east northeast or northeast was noted in Dinon et al. (2008). The updated climatology which includes over 800 warning and non-warning events (the previous study considered only 139 warning level events) is consistent with previous results, but shows a higher percentage of events, especially warning level, in the northeastward moving category (Figure 7). This is not surprising considering that the strongest convection in East Central Florida tends to occur when synoptic scale southwest flow at low and mid levels opposes the sea-breeze front enhancing convergence (Shafer and Fuelberg 2006). Warning level events have a component of group (individual cell) movement towards the east 81% (80%) of the time while non-warning level events have a component of group (individual cell) movement towards the east 44% (42%) of the time (Figures 7 and 8). This indicates that cells moving over the warm land tend to gain strength as they move east throughout the day and is also an artifact of the fact that much of the convection in East Central Florida occurs in the southwest flow regime (Figure 9). Non-warning level events tend to be more evenly distributed through the 16 cardinal directions of movement considered. Also of note is the peak in the variable/stationary category for non-warning level events. This is expected since a lot of the weaker, non-warning level events are likely caused by ordinary pulse thunderstorms that are associated with weaker, perhaps undetectable boundaries. Stronger events tend to be associated with mesoscale boundaries that generally have a distinguishable direction of movement.

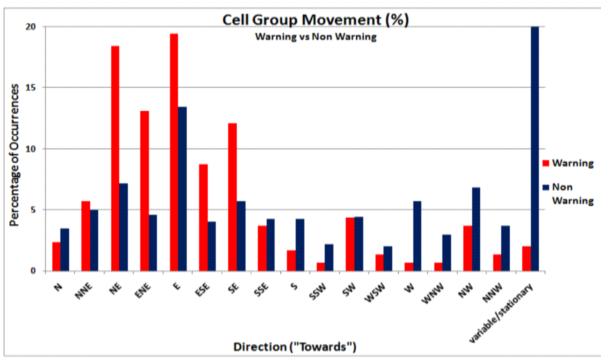

Figure 7. Cell Group Movement with warning level events in red and non-warning level events in blue. Direction towards is on the x-axis and percentage of occurrence is on the y-axis.

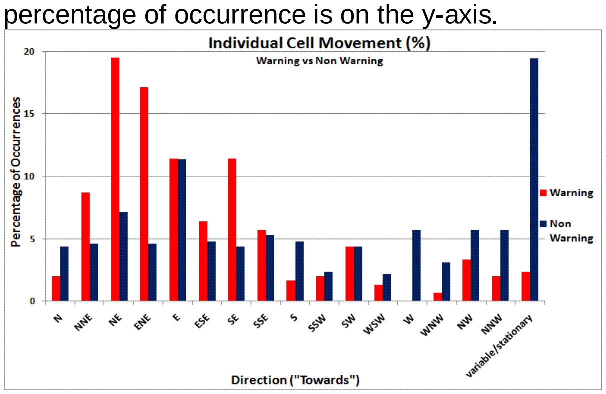

Figure 8. Same as Figure 6 but for Individual Cell Movement.

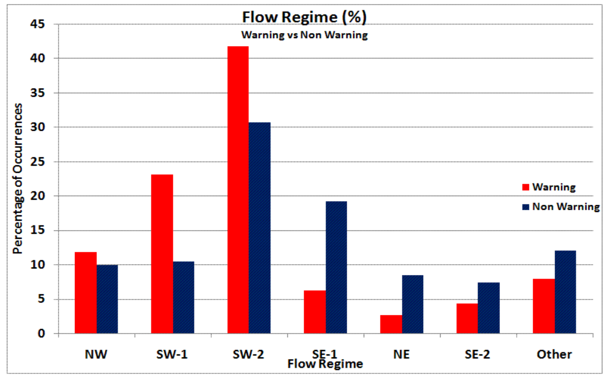

Figure 9. Percentage of occurrence of each flow regime for warning vs. non-warning level events.

5. Interface Examples/Case Study

In this section we will present the interface that was used to analyze events and also show examples of the collapsing core and a brief case study of the event that produced the maximum gust in the climatology.

5.1 Interface

The updated radar web interface, mentioned in section-3, is exemplified in figures 10 and 11. The particular case from 31 August 2005 was chosen because it clearly shows an interaction between a sea-breeze front and outflow boundary as well as an area of convergence likely associated with an updraft. Both the streamline analysis and the wind barbs show distinct wind shifts with the passage of each mesoscale boundary. Sea-breeze and outflow boundaries were more easily tracked using the wind barb interface while the streamlines were more useful for indentifying areas of convergence. This is due to the often complex orientation of the sea-breeze front as it follows the coastline (Lericos et. al. 2002). The streamlines have a tendency to smooth out this finer scale detail while the wind barbs will not.

5.2 Collapsing Core

On 29 August 2004 at 2100UTC a strong cell (≥55 dBZ) was approaching tower 397, located on the north east side of Cape Canaveral, from the west. This cell was the result of a collision between a sea-breeze front and an outflow boundary. The sea-breeze front and the diminishing cell that produced the outflow boundary can be seen just prior to collision at 2000Z (Figure 12). At 2100UTC, the now 55+ dBZ cell was located just to the southwest of tower

397. The cell is part of a line of cells oriented SSW to NNW that formed along the sea-breeze front and outflow boundary collision (Figure 13). At 2110UTC, five minutes prior to the occurrence of the max gust, the cell which had weakened slightly was located overhead of tower 397 (Figure 14). At 2115UTC tower 397 recorded the max gust of 48 kt and the cell which was still located overhead had undergone further weakening (Figure 15). By 2125UTC, the cell had moved east north east of tower 397 and had weakened considerably with maximum reflectivity values around 40dBZ. (Figure 16). This type of cellular development and degeneration was noticed frequently by the authors and, as previously mentioned; members of the 45 WS suggest that a time delay between the collapse of the cell core and the peak wind at the surface could be the cause.

6. Future Research

Upcoming research will focus on completing the climatological summary for all convective events, using RAOB data to examine current thermodynamic data for all warm season days, not just convective periods, fitting Gumbel curves to peak wind data and examining additional NEXRAD Strom Products data.

Gumbel curves have been fitted to the peak wind data for each month of the warm season however, there may be some value in separating the data by flow regime as there are now significantly more events in the database for each flow regime. Gumbel curves allow a probability of exceeding a given peak wind to be estimated based on climatology.

Other possibilities include time series statistics on the cell strength for a series of radar scans before the peak speed at the surface to see if the “delay” hypothesis is valid. In addition, this research project hopes to refine the radar maximum gust equation that regresses echo top, storm top, and VIL to predict the peak speed. Other parameters, such as VIL above the freezing level, could also be useful.

Another potential relationship of use is that between the difference in the height of maximum reflectivity and the freezing level vs. peak wind gust. Preliminary data based on 40 cases show that for stronger convective wind gusts (≥50 kt) the maximum reflectivity tends to be above the freezing level (Figure 17). More data are needed to develop a stronger relationship however many of the products needed for this are not available before 2004 for the KMLB NEXRAD site.

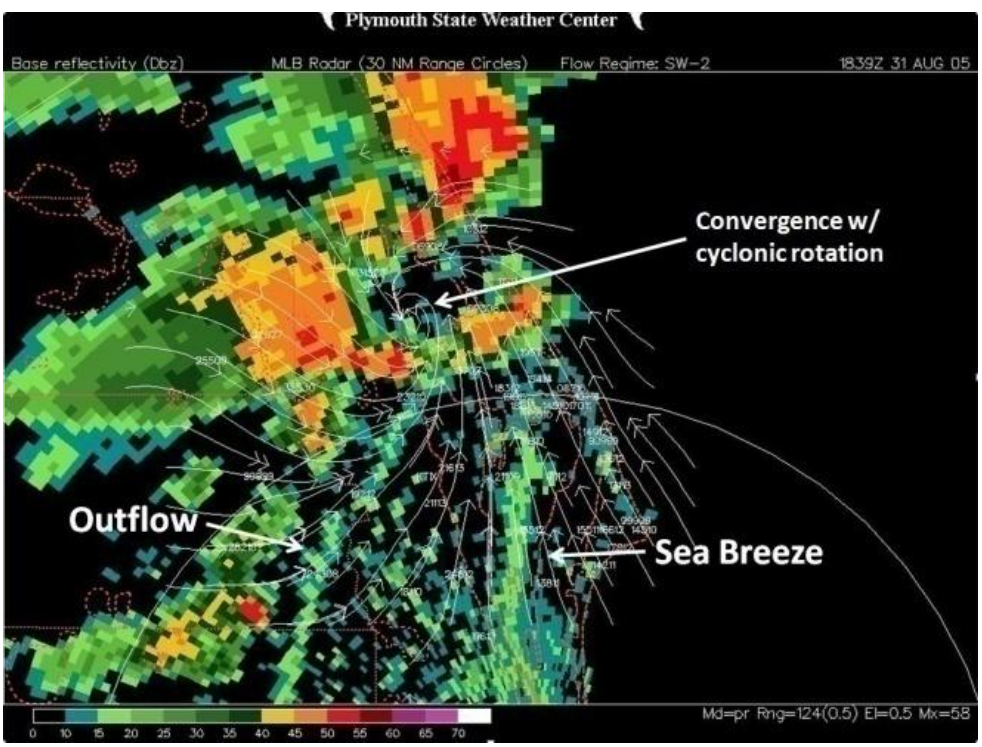

Figure 10. Example of the streamline analysis of time-matched peak winds overlaid with KMLB base reflectivity valid 31 August 2008 at 1839UTC.

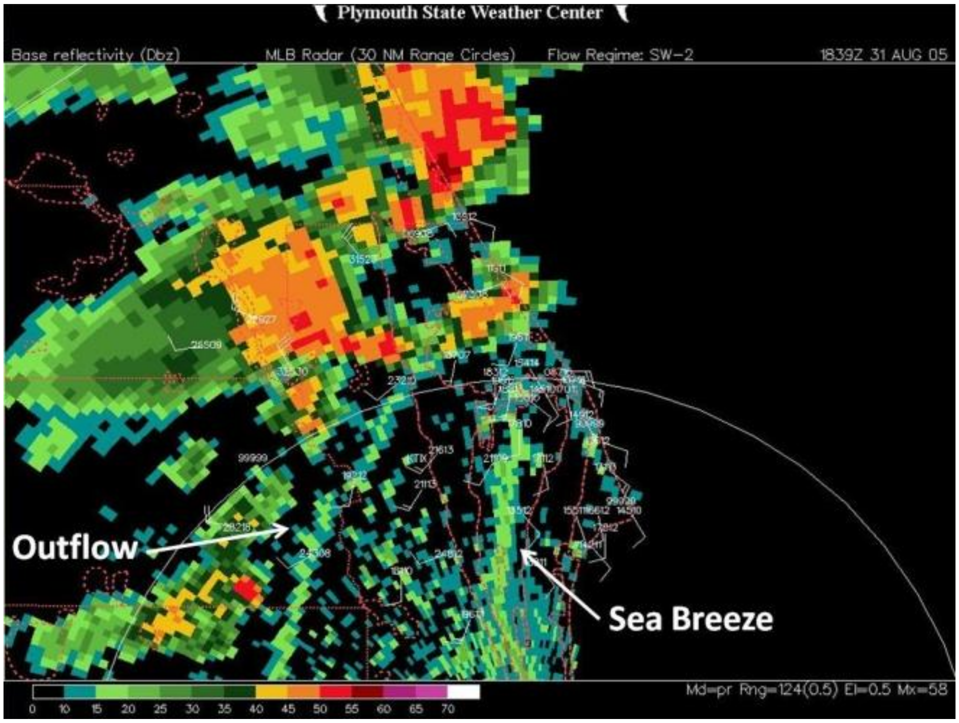

Figure 11. An example of a wind barb analysis of time-matched peak winds overlaid with KMLB base reflectivity valid 31 August 2008 at 1839UTC.

7. Summary

This paper has expanded on a previous radar study by Dinon et al. (2008) to include all convective events in the climatology with a focus on comparing and contrasting warning level events versus non-warning level events. Results show that sea-breeze front and outflow boundary interactions are important in the majority (68%) of warning level events. These boundaries tend to be quasi-linear resulting in linear cell structures for many of the warning level events. Some classifications such as cell strength presented interesting questions due to the fact that almost an equal percentage of warning and non-warning events fell into the weak/broken cell strength category. It was hypothesized that the collapsing of storm cores often observed just prior to peak gust led to lower reflectivity values being recorded than may have been present a few frames before the time of peak wind. In order to be consistent, cell strength was classified by looking at the maximum base reflectivity values in 3 frames; time of peak wind, five minutes prior to peak wind and five minutes after peak wind. A brief case study was presented to show the evolution of a cell that appeared to be "collapsing" as it approached the tower where the max peak wind was recorded.

Much more detailed data, analyses, and many of these and additional references for these studies are available online at the following URL:

http://vortex.plymouth.edu/conv_winds/

8. Acknowledgments

This work was supported through the NASA Space Grant Program under a University of New Hampshire Subcontract. We would also like to thank NCDC, the 14th Weather Squadron in Asheville, the Applied Meteorology Unit (AMU), and Computer Sciences Raytheon (CSR), who provided valuable archived data for our work. The Plymouth State University authors would also like to thank all personnel from the AMU and the 45 WS, who provided invaluable guidance while working at CCAFS during the summer of 2008.

9. References

Cummings, K. A., E. J. Dupont, A. N. Loconto, J. P. Koermer and W. P. Roeder, 2007. An updated warm-season convective wind climatology for the Florida space coast, *16th Conf. of Applied Climatology*, 14-18 Jan 2007.

Dinon, H. A., M. J. Morin, J. P. Koermer, and W. P. Roeder, 2008. Convective winds at the Florida Spaceport: year-3 of Plymouth State research, *13th Conf. on Aviation, Range, and Aerospace Meteorology,* 21-24 Jan 2008, New Orleans, LA.

Harms, D. E., A. A. Guiffrida, B. F. Boyd, L. H. Gross, G. D. Strohm, R. M. Lucci, J. W. Weems, E. D. Priselac, K. Lammers, H. C. Herring and F. J. Merceret, 1999: The many lives of a meteorologist in support of space launch, *8th Conf. On Aviation, Range, and Aerospace Meteorology,* 10-15 Jan 99, Dallas, TX, 5-9.

Koermer, J. P., and W. P. Roeder, 2008: Assessment of the importance of certain wind towers in the Cape Canaveral AFS/Kennedy Space Center mesonet for predicting convective winds, *13th Conf. On Aviation, Range,And Aerospace Meteorology,* 21-24 Jan 08, New Orleans, LA.

Lambert, W. and W.P. Roeder, 2008: Update to the Lightning Probability Forecast Equations at Kennedy Space Center/Cape Canaveral Air Force Station, Florida, *2nd International Lightning Meteorology Conf., 24-25 April 2008, 16pp.*

Lericos, T. P., H. E. Fuelburg, A. I. Watson, and R. I. Holle, 2002. Warm season lightning distributions over the Florida Peninsula as related to synoptic patterns. *Weather and Forecasting*, 17, 83-98.

Loconto, A. N., 2006: Improvements of warm-season convective wind forecasts at the Kennedy Space Center and Cape Canaveral Air Force Station. *M.S. Thesis*, Dept. of Chemical, Earth, Atmospheric and Physical Sciences, Plymouth State University, Plymouth, NH.

Loconto, A. N., J. P. Koermer, and W. P. Roeder, 2006: An updated warm-season convective wind climatology for Cape Canaveral Air Force Station/Kennedy Space Center, *12th Conference on Aviation Range and Aerospace Meteorology*, 30 Jan–2 Feb 2006, in Combined Preprint CDROM.

Shafer, P.E., and H.E. Fuelberg, 2006: A Statistical Procedure to Forecast Warm Season Lightning over Portions of the Florida Peninsula. *Wea. Forecasting*, **21**, 851–868.

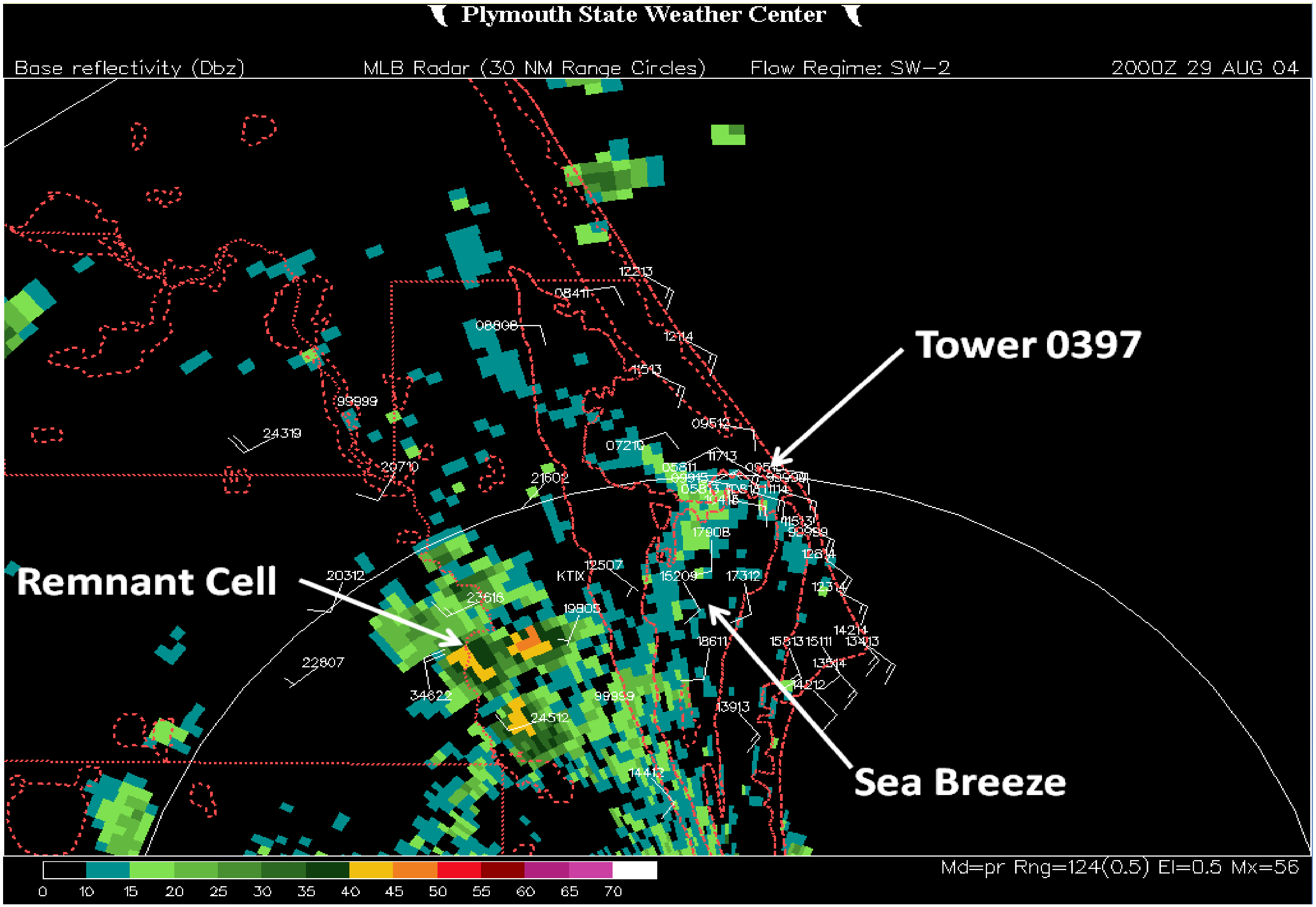

Figure 12. Radar/Wind depiction for 29 August 2004 at 2000UTC shows cell initiation along the sea-breeze front and an outflow boundary from the remnants of earlier convection.

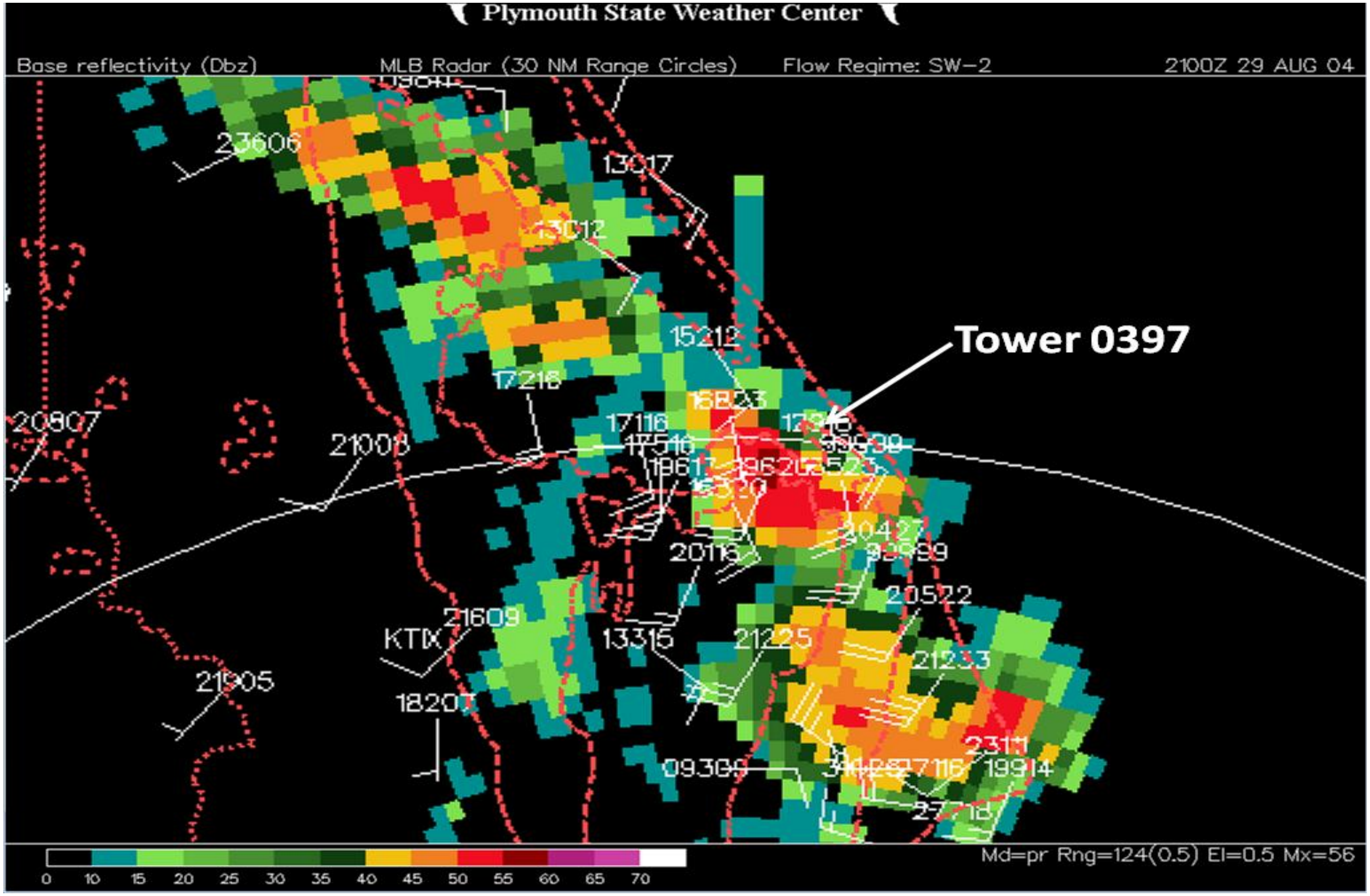

Figure 13. Radar/Wind depiction for 29 August 2004 at 2100UTC zoomed in on strong cell 15 minutes prior to the maximum peak wind gust at tower 0397.

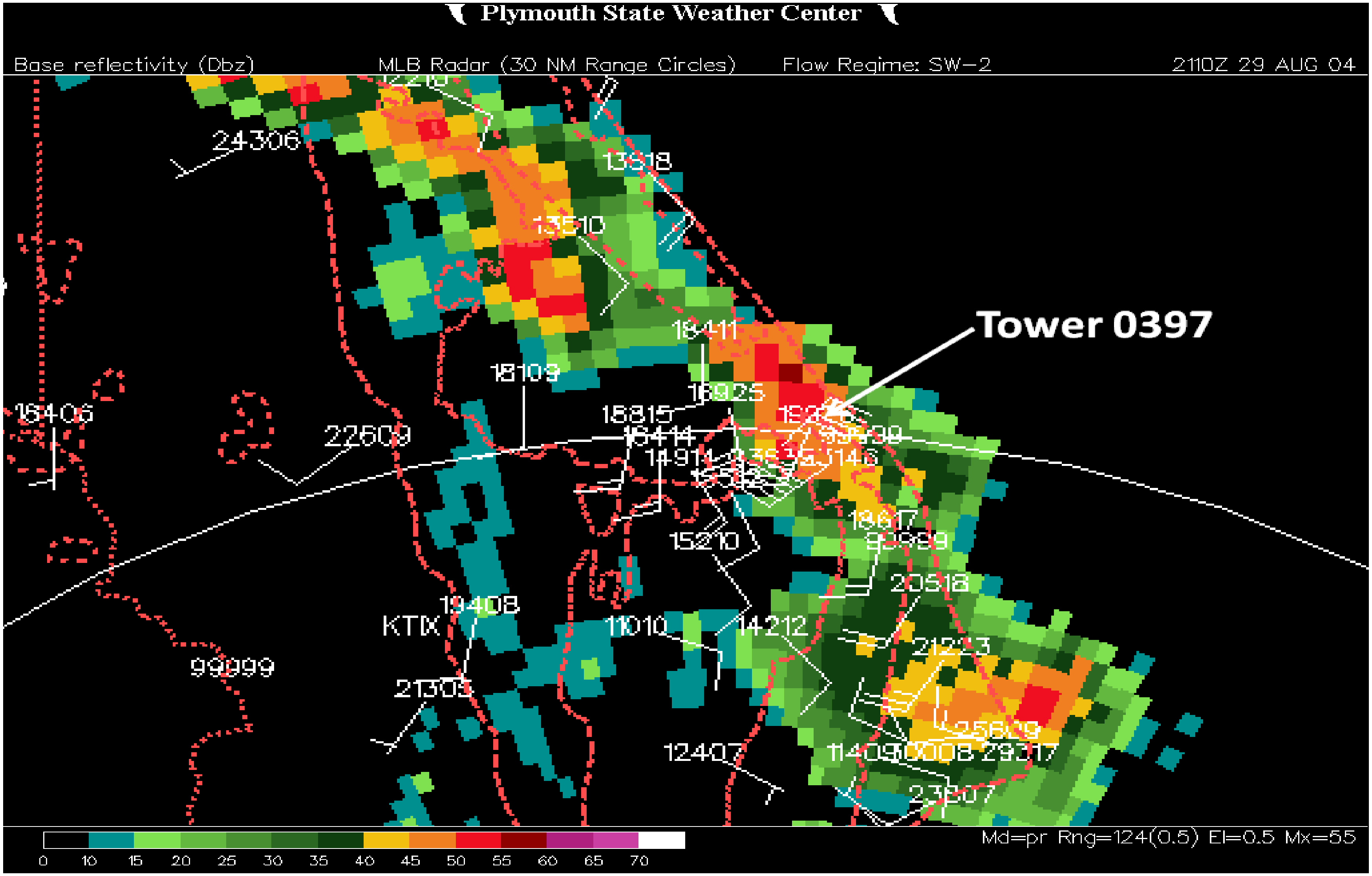

Figure 14. Radar/Wind depiction for 29 August 2004 at 2110UTC, which was 5 minutes prior to maximum peak wind gusts, shows a strong cell just over head and a maximum gust of 26 kt at tower 0397.

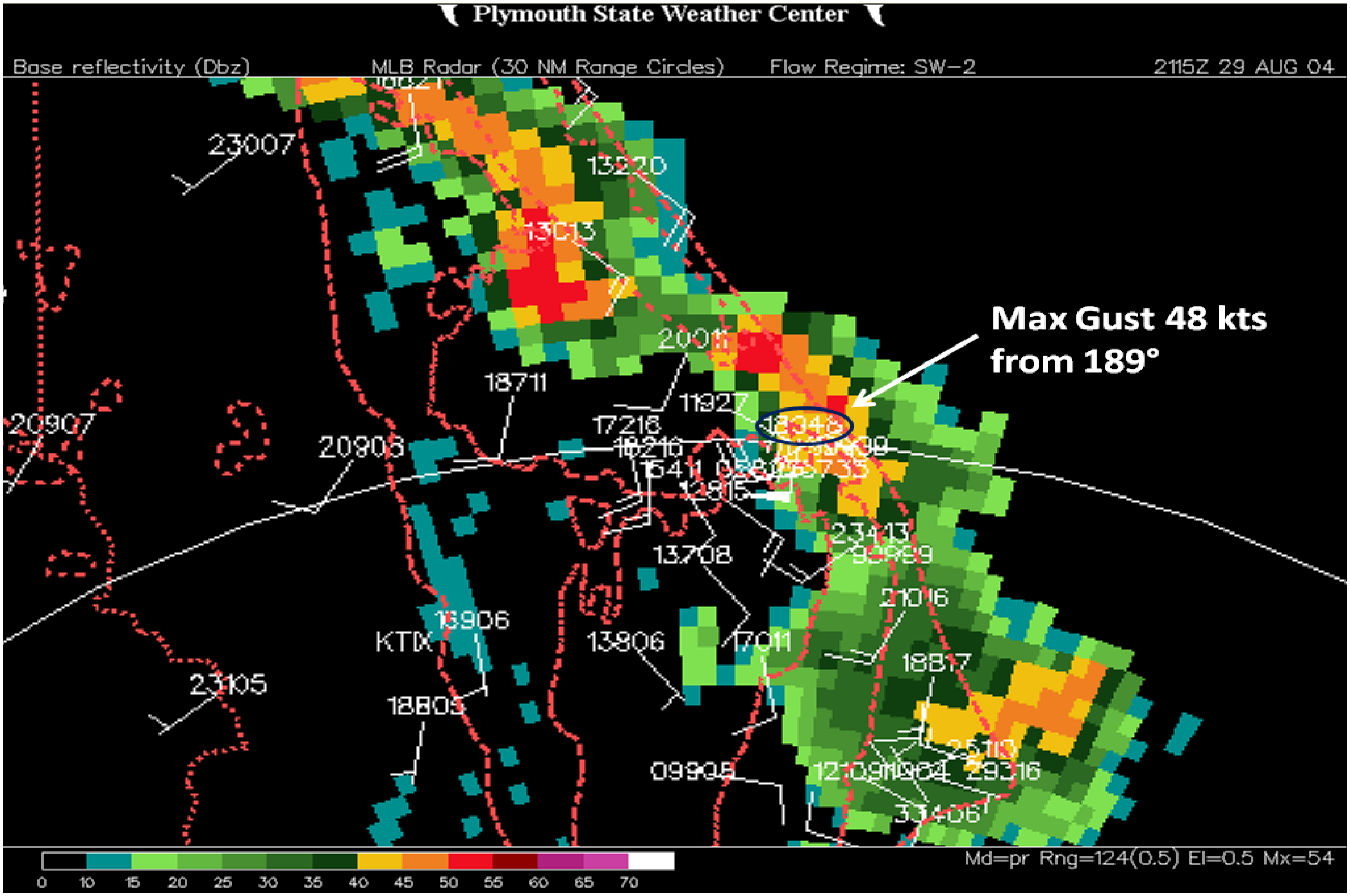

Figure 15. Radar/Wind depiction for 29 August 2004 at the time (2115UTC) of peak gusts shows slightly lower reflectivity values directly over tower 0397 indicating that the cell has started to weaken.

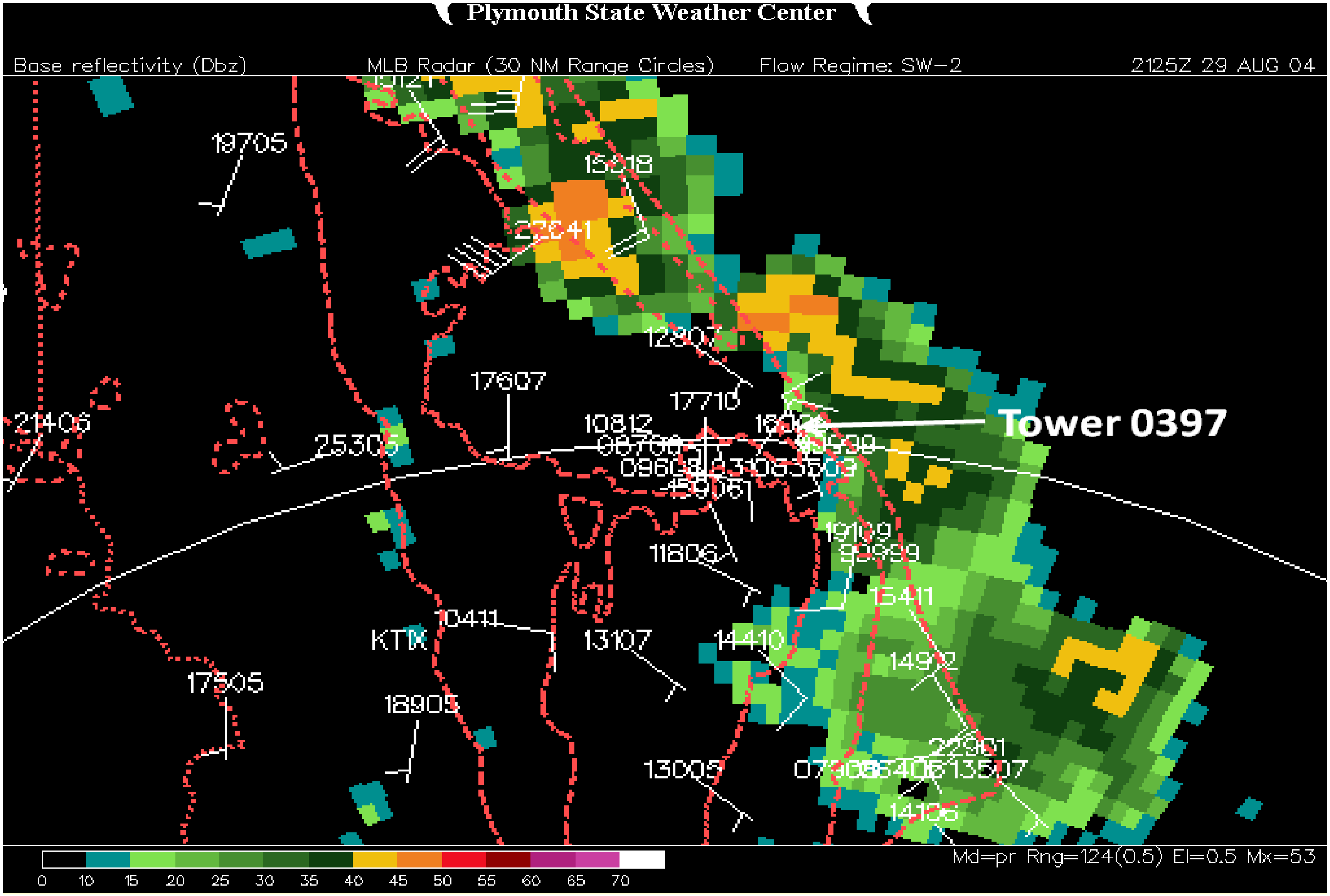

Figure 16. Radar/Wind depiction for 29 August 2004 at 2125UTC shows that the cell has weakened significantly just 10 minutes after producing the peak wind gust.

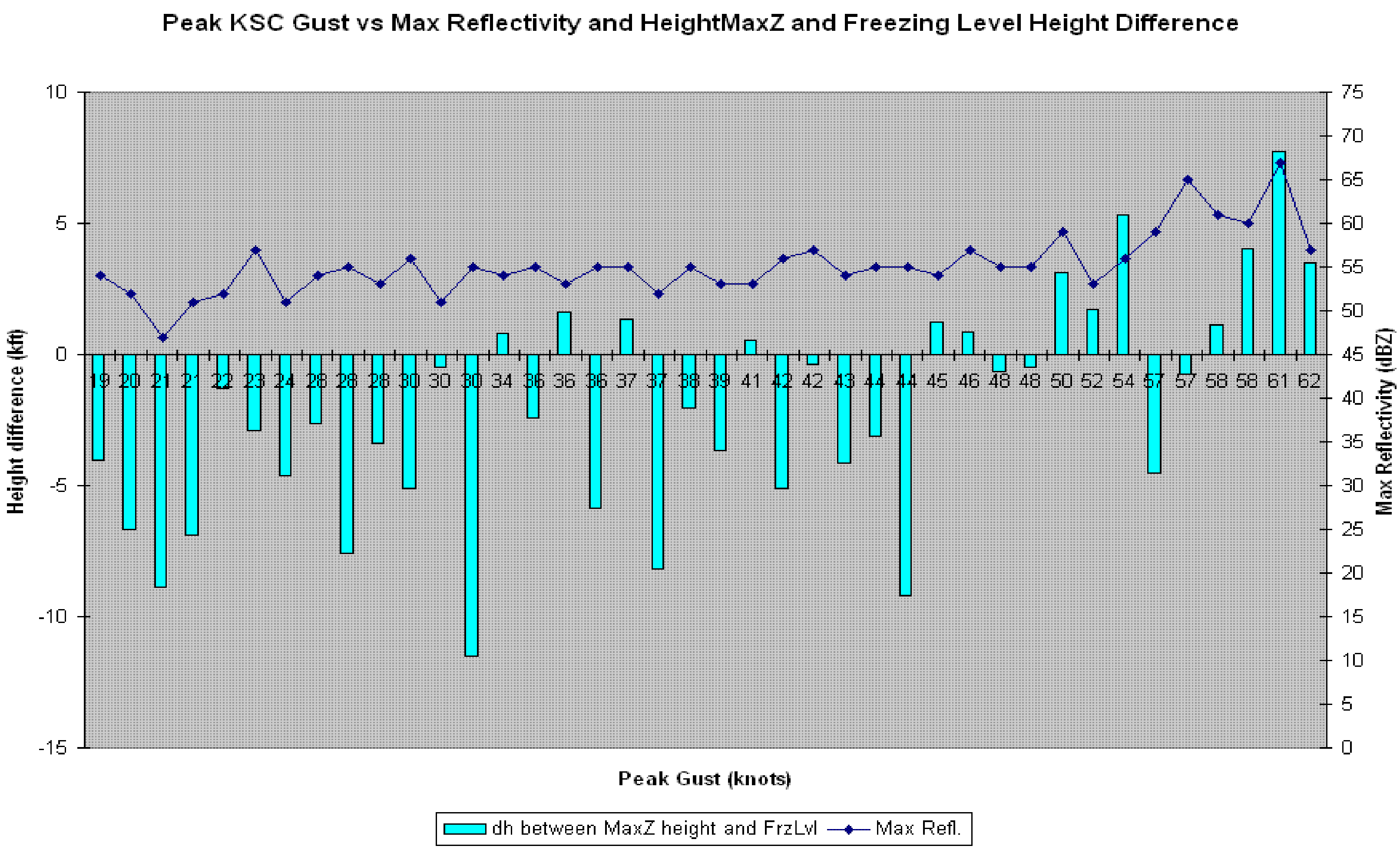

Figure 17. The x-axis shows observed peak wind gusts. On the y-axis, blue points show the corresponding maximum reflectivities in dBZ, while the aqua bars show the height differences in thousands of feet between the height of the maximum and freezing level. Bars with values greater (less) than zero indicate a maximum reflectivity located above (below) the observed freezing level. (from Loconto 2006).